

FACIAL EXPRESSION RECOGNITION USING MULTI-STRUCTURE LOCAL BINARY PATTERN

T.Sabhanayagam¹, Dr.V.Prasanna Venkatesan²

Dr. K.Senthamaraikannan³

¹Research Scholar, Center for Computer and Information Technology Engineering,
Manonmaniam Sundaranar University, Tirunelveli, Tamilnadu (India)

¹And Assistant Professor, School of Computing, SRMSIT, Chennai

²Prof & Head, Dept. of Banking Technology, Pondicherry University, Puducherry (India)

³Prof & Head, Dept. of Statistics,

Manonmaniam Sundaranar University, Tirunelveli, Tamilnadu (India)

ABSTRACT

In facial expression recognition, the local binary patterns (LBP) are broadly employed. The LBP techniques gather the binary patterns by correlating the gray scale pixels on small circularly neighbourhood area with the center pixel. The traditional LBP techniques define only the micro structures of the facial images, even though the multi-resolution strategy is used and they are not able to define the macro structures of the facial image. This paper suggests an extended LBP by changing the shape of the sampling region. A multi-structure local binary pattern (Ms-LBP) is accomplished by applying the extension of LBP operator on various of a pyramidal image. Hence, the suggested technique is efficient and simple to define four types of structures of facial image: anisotropic microstructure, isotropic microstructure, anisotropic macrostructure and isotropic macrostructure. The performance of technique is evaluated on the databases: JAFFE and Cohan-Kanade and the results show the merits of the suggested technique.

Keywords: Local Binary Pattern, multi-structure, facial expression, microstructures, macrostructures, anisotropic

I. INTRODUCTION

Designing an automated facial expression recognition system environment to have the human at the center of the system is a great challenge. The system should be able to associate the user in a common way for the genuine Human-Computer Intelligent Interaction Systems (HCII) and it should define non-verbal behaviour such as body gesture, voice and facial expression to recognize the emotions. The facial expression is the common way of disseminating human feelings, opinions and intentions to each other. Facial expression takes part significant role in disseminating motives and feelings. A. Mehrabian [1] showed that 55% of feelings are expressed by facial expression alone and 7% of spoken words and 38% of voices of information communicated separately. Ekman et al. [2] done a psychological research on facial expression and they inferred that there are six universal facial expressions includes Happiness, Sadness, Disgust, Anger, Surprise and Fear (shown in

figure 1). Face detection, features extraction and classification are the three essential parts of Facial expression recognition. Visual information and cues lead to superior comprehension in a conversation. FER covers wide range of applications, including physical pain reviewing, detection of smile [3],[4],[5], detection of tiredness [6], assessment of patient pain [7], robotics, video indexing and virtual reality [8], detection of dejection [9] and so forth. The state of mind is reflexed on the face in the way of different expressions and these expressions are modelled into an appropriate action by affective computing [10]. Facial expression interpreted using computer become main thrust for future automated interfaces, for example robotics, Human-Computer Interfaces, car driving, driver alert systems and so on [8],[11]

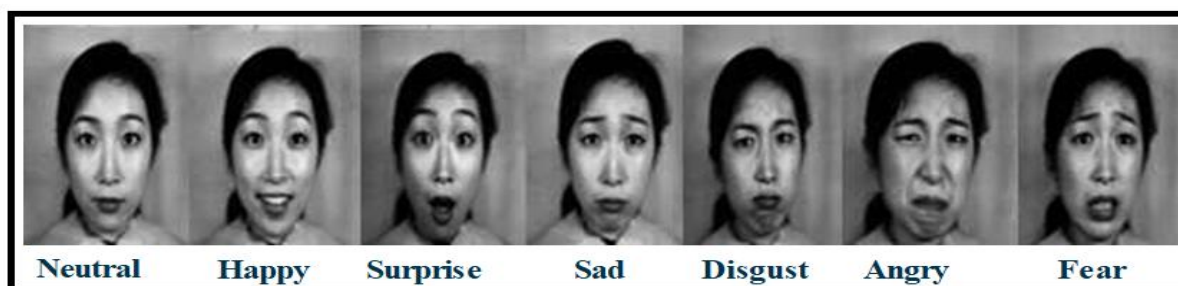


Fig. 1 Basic Facial Expressions (JAFPE)

II. RELATED WORK

The analysis of texture is considered as the most significant parts of Computer Vision and acts as a vital role in various application, for example surface analysis [12], content-based image retrieval [13], medical imaging [14] and so on. Amid the past few decades, texture classification has been widely explored, particularly the textures that are acquired under various conditions.

The earlier approach for texture classification includes the co-occurrence matrix method [15] and filtering-based methods [16–[18]. These approaches are impressionable to the illumination and the rotation variations.. Lately, numerous filtering methods construct textons for the extraction powerful texture features. Leung and Malik [19] developed 3D textons acquired under various conditions from a heap of texture images for classifying the structures. Schmid [20] utilized isotropic “Gabor-likes” filters to construct textons for rotation-invariant classification of texture from a single image.

Varma and Zisserman [21] devised a valuable statistical algorithm, MR8, to construct a rotation invariant texton library with help of 38 filters from a training set for categorizing a new image. The Local Binary Pattern (LBP) [22] acquires attributes by mapping the surrounding gray scale pixels in neighbourhood area, different from the texton-based technique. It has been effectively used to various areas, for example, texture analysis [23], [24], region description [25], facial recognition [26]–[29] and so forth.

For the classifying the texture, Ma^{enpa} et al. [30] proposed the uniform patterns to improve the description of texture by choosing a part of patterns encoded in the form of LBP. Using this technique, they suggested uniform pattern (LBP^{riu2}) operator [31] to define rotational textures, which is a rotationally-invariant. Liao et al. [32] utilized the Dominant Local Binary Patterns (DLBP) for rotational classification of texture and used the SVM to improve the efficiency. Ahonen et al. [33] used the frequency domain by translating the histogram of uniform

LBP and suggested the Local Binary Pattern Histogram Fourier features (LBP-HF) to define the textural patterns.

The local variances are used by Guo et al. [34] for assigning weights to uniform patterns and suggested the LBPV operator. The feature histograms are generated in all possible orientations by rearranging sequence of bins of LBPV histogram for categorizing rotational textures. Afterwards, they [35] suggested a completed modeling of the LBP operator (CLBP_S/M/C) that integrates three parts of local information: local signs (CLBP_S), local magnitudes (CLBP_M) and center grays (CLBP_C), Using the information of temporal domain, Zhao and Pietikainen [36] suggested the Volume Local Binary Patterns (VLBP) for dynamic classification of texture by extracting the local binary patterns from three orthogonal planes (LBP-TOP). Though the LBP techniques perform well, majority of the binary patterns involves the patterns in smaller neighbourhoods and extract only the microstructures of the images. But these microstructures are not sufficient to define the textural information. Still there exists a problem even after applying the multi-resolution technique [31]. It just fuses surrounding pixels and radii in limited manner. These sampling radii should be small since the increase in neighbourhood radii degenerate the stability of LBP quickly.

Maenpa and Pietikainen [37] suggested the LBPF operator to extract bigger structures under the original version of the LBP technique. For texture analysis, to extract the binary pattern, the LBPF utilized Gaussian low-pass filtering and exponentially growing circularly neighborhoods. The LBPF also exhibits isotropic microstructures, since the diameter of circularly neighborhood is restricted by the neighbourhood radii. Turtinen and Pietikainen [38] extracted the LBP feature for the classification of sense with three scales and are restricted to various mutually disjoint regions. Qian et al. [39] suggested the PLBP operator by placing the original LBP on pyramidal image and it recognizes the isotropic information. Furthermore, the achievement of the PLBP is restricted by the high level patterns of the pyramidal image and it could cause adverse effect, when a more number of sampling pixel points is accessible.

In Multi-Structure LBP (Ms-LBP), the pyramid of image is also used to generate the neighbourhood regions with distinct sizes. To depict isotropic and anisotropic structures, two types of LBP are utilized. One LBP uses the surrounding pixels on a circular neighbourhood and the other one uses the elliptical neighbourhood with four distinct rotating angles and the elliptical LBP is susceptible to sample's rotating angles. Liao et al. and Nanni et al. [27, 40] also used the elliptical LBP without considering the problem of rotation-variant.

In order to construct the feature histogram in possible orientations, the ordering of the obtained feature histograms can be adjusted by mapping the extracted features in all the possible related orientations. In a pyramidal image to capture both micro and macrostructures of textural images, uniform LBP is carried out. In Ms-LBP, four kinds of structures are defined: anisotropic microstructure, isotropic microstructure, anisotropic macrostructure and isotropic macrostructure and to improve the performance of the proposed technique, the histograms of various obtained information are provided with the weights properly.

II. THE LBP METHODS

The LBP technique [20] describes the neighbourhood pixels of the textural image. It uses a simple circular neighborhood P uniformly distributed on a circle with R of radius. Figure 1 shows distinct

neighbourhoods (P) and radii (R). The center pixel's value in LBP is calculated by thresholding the neighbouring point with respect to the center, and sums the thresholded values by multiplying the binary weights. Thus, the LBP value for the center point of pixel (x, y) is defined by

$$LBP_{P,R}(x, y) = \sum_{p=0}^{P-1} s(g_p - g_c) 2^p$$

$$s(x) = \begin{cases} 1, & x \geq 0 \\ 0, & x < 0 \end{cases}$$

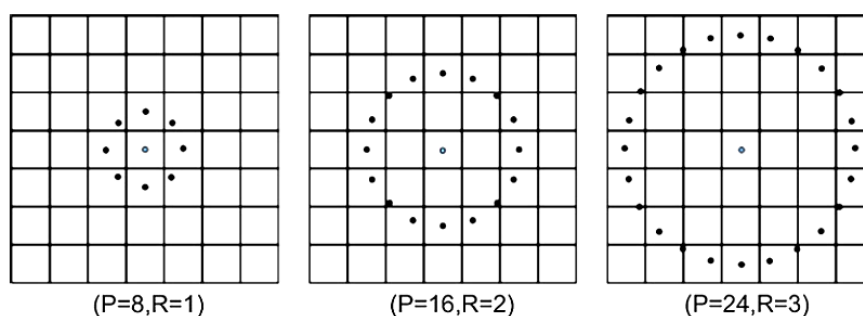


Fig. 2 Circularly symmetric neighborhoods for distinct (P,R)

where g_c denotes the value of the centre point pixel; g_p ($p = 0, \dots, P - 1$) represents the value of the p^{th} neighbouring sample points. If (0, 0) are the values for g_c , then values of g_p are defined by $(-R \sin(2\pi p/P), R \cos(2\pi p/P))$. The neighbouring points which do not fall absolutely on the grid's center are determined by the interpolation. The original LBP is receptive to the orientations. Ojala et al. [20] nominate the patterns as the uniform patterns whose 0 to 1 or 1 to 0 transitions are 2 at most and suggest the rotation-invariant uniform pattern operator $LBP_{P,R}^{\text{riu2}}$

$$LBP_{P,R}^{\text{riu2}} = \begin{cases} \sum_{p=0}^{P-1} s(g_p - g_c) & \text{if } U(LBP_{P,R}) \leq 2 \\ P + 1 & \text{otherwise} \end{cases}$$

where

$$U(LBP_{P,R}) = |s(g_{P-1} - g_c) - s(g_0 - g_c)| + \sum_{p=1}^{P-1} |s(g_p - g_c) - s(g_{p-1} - g_c)|$$

As per the definition of 'uniform', there exists $P+1$ 'uniform' binary patterns in a circularly symmetric neighbor set of P pixels and each of them assigned with a unique label, corresponding the number of '1' bits in the pattern (0, 1, ..., P) and all the 'non-uniform' patterns are bring together under the label (P+ 1). Thus, the $LBP_{P,R}^{\text{riu2}}$ has $P + 2$ distinct output values.

3.1 Drawback of the Conventional LBP

The LBP techniques simply calculate the patterns on small local areas and patterns extracted from them define the micro structures of images, for example flat region, corners, edges, spots etc. The histogram of LBP image is constructed from the occurred frequency of these micro structures. Since the traditional LBP rely only upon the micro structures of images, their performance is restricted. Even the uniform LBP are used to define the problem, all the conventional LBP techniques have the same kind of conclusion. Thus, it is clear from the fact the LBP having similar feature histograms cannot be even classified by the uniform patterns since some essential information may be lost by the conventional LBP techniques which simply concentrate on microstructure of images.

IV. MULTI-STRUCTURE LOCAL BINARY PATTERN

The original LBP concentrates on the isotropic microstructures only. To extract both anisotropic and isotropic LBP, the shape of the sampling area is to be changed. It is carried out on pyramidal image to define four distinct forms of structures: (1) anisotropic microstructure; (2) isotropic microstructure; (3) isotropic macrostructure; (4) anisotropic macrostructure.

4.1 Extended LBP

The traditional LBP techniques obtain the neighbourhoods in a circular area, useful for acquiring the isotropic data. Here, the shapes of neighbourhood areas are altered to define both anisotropic and isotropic structures. The neighbouring pixels are derived not only from the circular area, also from four elliptical neighbourhood areas. All the four ellipses are the similar, only differs in angle of rotation θ : 0° , 45° , 90° and 135° . For every ellipse, the proportion of its minor and major axis is constrained to 2:1 and the length of the minor axis of an ellipse should be equal to the radius of the circle. Still R is the radius used to express the size of the ellipse. Assume that the center pixel coordinate of the elliptical LBP is $(0, 0)$. Then the coordinates of the p^{th} neighbourhood point (x, y) are equal to

$$\left. \begin{aligned} 2R \cos(2\pi p/P + \theta) \cos(\theta) + R \sin(2\pi p/P + \theta) \sin(\theta), \\ -2R \cos(2\pi p/P + \theta) \sin(\theta) + R \sin(2\pi p/P + \theta) \cos(\theta). \end{aligned} \right\} \begin{array}{l} \text{x - coordinate} \\ \text{y - coordinate} \end{array}$$

Figure 3 shows the five types of structures with eight neighbourhoods. The operator $LBP_{P,R}^{riu2}$ can be modified as $LBP_{T,P,R}^{riu2}$ and is defined as

$$LBP_{T,P,R}^{riu2} = \begin{cases} \sum_{p=0}^{P-1} s(g_p - g_c) & \text{if } U(LBP_{T,P,R}) \leq 2 \\ P + 1 & \text{otherwise} \end{cases}$$

where 'T' represents the sampling type and $T \in \{0, 1, 2, 3, 4\}$. $T = 0$ represents the circular neighbourhood area, whereas $T = 1, 2, 3, 4$ uses elliptical neighbourhood area with angles of rotation 0° , 45° , 90° and 135° respectively.

4.2 Image Pyramid

An image pyramid is formed from the original image. The symbol I_l is used to denote the sub-images of the pyramid and l represents the level of the pyramid. While constructing the pyramidal image, the Gaussian

function $G(x, y, \sigma)$ is applied for image smoothing. As stated in the SIFT operator [42], the variance value $\sigma = 1.5$ can be chosen.

$$G(x, y, \sigma) = \frac{1}{2\pi\sigma^2} e^{-(x^2+y^2)/2\sigma^2}$$

Assume that I_0 is the original image. Then I_l , the sub-image is constructed from the image I_{l-1} using the formula:

$$I_l = (I_{l-1} * G) \downarrow 2$$

where $*$ is the convolution operation and $\downarrow 2$ is the down sample by 2. The three-levels of pyramid image of extracting distinct structures is shown in Figure 4.

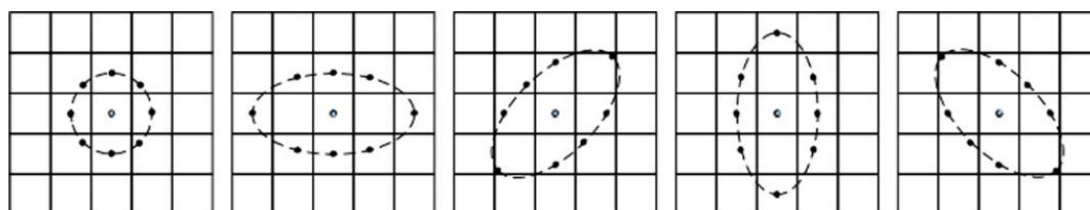


Fig. 3 Types of neighbourhood with $(P, R) = (8, 1)$

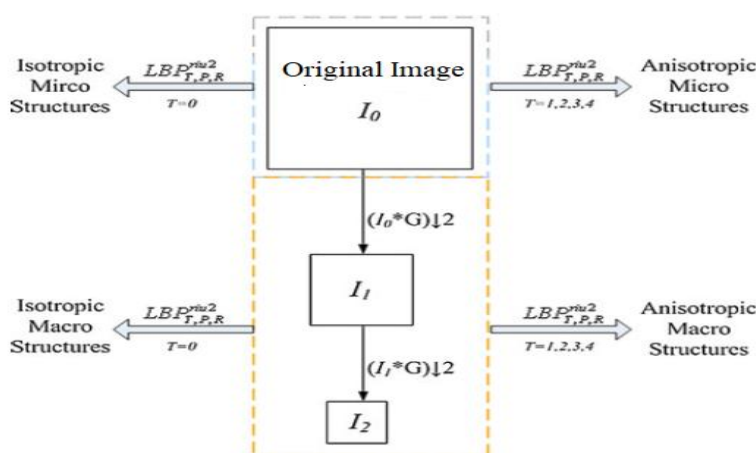


Fig. 4 Extraction of Multi-structures from pyramid with three levels.

4.3 Multi-Structure Local Binary Pattern Feature

The Ms-LBP) Multi-structure Local Binary Pattern (Ms-LBP) can be accomplished by applying the $LBP_{T,P,R}^{riu2}$ operator pyramid image. The isotropic microstructures are acquired by applying operator $LBP_{T,P,R}^{riu2}(T=0)$ on the original image, whereas the anisotropic microstructures are acquired by applying the operators $LBP_{T,P,R}^{riu2}(T = 1, 2, 3, 4)$ on the same original image. Similarly, by applying the operator $LBP_{T,P,R}^{riu2}(T=0)$ on the sub-images I_l ($l > 0$), the isotropic macrostructures are captured and the anisotropic macrostructures are captured by applying the operators $LBP_{T,P,R}^{riu2}(T = 1, 2, 3, 4)$ on the sub-images I_l ($l > 0$). For regularity, it can be denoted as Ms- $LBP_{P,R}^{riu2}$, where the symbols 'P', 'R' and 'riu2' have the same meaning in the operator $LBP_{P,R}^{riu2}$.

The final feature histogram of the Ms-LBP_{T,P,R}^{riu2} along with LBP_{T,P,R}^{riu2} histograms of each single sub-images of the pyramidal image:

$$H_{l,T}(k) = \sum_{i=1}^N \sum_{j=1}^M f(\text{LBP}_{l,T,P,R}^{\text{riu}2}(i,j), k), \quad k \in [0, K]$$

$$f(x, y) = \begin{cases} 1 & x = y \\ 0 & \text{otherwise} \end{cases}$$

where LBP_{T,P,R}^{riu2}(i, j) is the LBP_{T,P,R}^{riu2} value of the pixel I_l (i, j); K is the maximal LBP_{T,P,R}^{riu2} pattern; H_{l,T} is the histogram of LBP_{T,P,R}^{riu2} of the sub-image I_l; M and N are the sizes of the sub-image of the pyramidal image.

4.4 Classification Principle

Numerous techniques are available to find the dissimilarity between a model and a sample. The Chi square distance measure is one of the valuable measures, which is used by many studies [19, 21, 34, 35, 43] in the classification of texture. The Chi-square distance between a sample S and a model M is defined as follows:

$$D(S, M) = \sum_{b=1}^B \frac{(S_b - M_b)^2}{S_b + M_b}$$

where B is the number of bins; M_b and S_b represents the model and the sample values at the bth bin, respectively. In comparison with the microstructures, the macrostructures are situated in top of the pyramid give little statistics as the smaller size of sub-images are at higher levels. Apparently, in the pyramidal image, the higher levels provide fewer information than the lower levels. The final dissimilarity distance (D_F(S, M)) is computed by summing all the distances of histograms with various weights in different level:

$$D_F(S, M) = \sum_{l=0}^L w_{l,0} D(S_{l,0}, M_{l,0}) + \sum_{l=0}^L w_{l,1} D_{\min}(S_l^{\text{an}}, M_l^{\text{an}})$$

$$\begin{cases} D_{\min}(S_l^{\text{an}}, M_l^{\text{an}}) = \frac{1}{4} \sum_{T=1}^4 D(S_{l, \text{mod}(T+k-1,4)+1}, M_{l,T}) \\ k = \arg \min_j \left(\sum_{l=0}^L \sum_{T=1}^4 D(S_{l, \text{mod}(T+j-1,4)+1}, M_{l,T}) \right), \quad j = 0, 1, 2, 3 \end{cases}$$

where S_{l,T} and M_{l,T} represents the LBP_{T,P,R}^{riu2} histogram of sample and model, in the lth level of the pyramid, respectively; the distant weights of the anisotropic and the isotropic parts in the lth level of the pyramid are denoted by w_{l,0} and w_{l,1} respectively; the topmost level of the pyramid is represented by L; k represents the anisotropic histograms correlating the angle of rotation with respect to the samples; D_{min}(S_l^{an}, M_l^{an}) is the sum of the distances of anisotropic structures between the original M_{l,T} and the adjusted S_{l,T}.

The percentage of classification is an excellent aspirant for the distant weight and it should be computed from the set of training samples. From each class, one sample is selected and in turn, form a new training set using selected samples, while other samples are utilized for testing. The anisotropic and isotropic features are acquired

in every pyramid level for each test group. Each feature in every level of the pyramid is utilized during classification of the texture in the created testing group.

For the isotropic structures, the essential Chi-square distance is utilized to find the dissimilarity of the isotropic histograms. For the anisotropic structures, the best oriented direction is only sought from the present level of the pyramid. Thus, the anisotropic dissimilar distance is given by

$$D(S_l^{an}, M_l^{an}) = \min_k \left(\frac{1}{4} \sum_{T=1}^4 D(S_{l, \text{mod}(T+k-1,4)+1}, M_{l,T}) \right),$$

$$k = 0, 1, 2, 3$$

The percentage of classification is different for distinct structures. For each structure, the mean rate of classification depends on its corresponding weight. In the pyramidal image, the sub-images provide more information since they are at lower levels and so weight of $1/2^l$ is set to the l^{th} level of the pyramid provide incredible information. The distant weights are chosen as the combined weights of the structure and the pyramid and all the final distant weights are standardized and summed one.

V. EXPERIMENTAL RESULTS AND DISCUSSION

The efficiency of the suggested work is evaluated for CK[44] and JAFFE [45] datasets using Chi-square distance measure, histogram normalized measure and SVM. CK dataset consists of 97 university students' image sequence having male and female in the ratio of 7:13 respectively. The people are in the age group of 18-30 years. Each subject performed serial of 23 face displays.

The JAFFE data is mainly used for facial expression recognition systems. It consists of 213 images of 10 Japanese female, with 3 or 4 subjects of each of the 7 basic expressions. The details of images from these datasets utilized for the experiment are given in Table 1.

Table 1. Total number of images utilized for the experiment from each dataset.

	Anger	Disgust	Fear	Happy	Surprise	Sad	Neutral	Total
CK	110	120	100	280	130	220	320	1280
JAFFE	30	29	32	31	31	30	30	213



Fig. 2 Snapshots from the databases CK and JAFFE

Table 2 Confusion Matrix for CK datasets

CK	Anger (%)	Disgust (%)	Fear (%)	Happy (%)	Sad (%)	Surprise (%)	Neutral (%)
Anger	96.3	0.1	1.2	0.4	1.2	1.2	0.4
Disgust	0.9	97.2	0.8	0.2	0.6	0	0.3
Fear	0.8	0.2	98.8	0	0.2	0	0
Happy	0.2	0.1	0.4	99.1	0.2	0	0
Sad	0.6	0.3	0.3	0.1	98.1	0.1	0.5
Surprise	0.2	0.1	0.2	0.1	0	99.4	0
Neutral	0.4	0.4	0.1	0.1	0.7	0.1	98.2
Average	98.2						

From the tables 2 and 3, the expressions surprise and happy are distinguishable when comparing with other expressions. During the surprise, maximum facial muscle deformations happen. Experimental results also demonstrate that the expressions surprise and happy expressions have better recognition rate comparing to other. Often there is a confusion between angry and fear and similarly for sad and disgust and have higher rate of false recognition. The classification of Facial expression is a multi-class problem. The functionality of basic binary SVM is extended to the multiclass problem

Table 3 Confusion matrix for JAFFE data sets

JAFFE	Anger (%)	Disgust (%)	Fear (%)	Happy (%)	Sad (%)	Surprise (%)	Neutral (%)
Anger	85.4	4.5	3.6	1.5	2.5	1	1.5
Disgust	2.9	84.7	5.1	1.5	3.5	1.2	1.1
Fear	3.5	2.3	87.4	1.2	3.2	1.1	1.3
Happy	2.5	1.4	2.7	90.6	0.8	1.2	0.8
Sad	4.2	2.6	2.5	0.9	86.3	0.3	3.2
Surprise	1.6	1.4	2.1	1.1	0.7	92.3	0.8
Neutral	1.7	1.8	2.7	0.9	3.2	0.5	89.2
Average	88.0						

The performance of Ms-LBP feature descriptor is compared with the recent state of the art methods. Since CK and JAFFE are designed under a controlled environment, it is not complex to localize the features after registration of face. The success of expression recognition systems also depends on the ethnic difference. Subjects belonging to JAFFE are in same ethnicity, whereas in CK 15% of subjects are from African-American

and 3% subjects are from Asian or the Latino-American .The performance of Ms-LBP with various methods is compared in Table 3 for the used datasets.

Table 4 Performance comparison with state of the art methods

Dataset	[47]	[48]	[46]	[49]	[50]	Ms-LBP+ Chi-Square	Ms-LBP+ SVM
CK	88.9	93.4	94.1	45.7	96.6	98.2	99.3
JAFFE	80.7	84.9	91.8	95.2	98.8	88	90.3

VI. CONCLUSIONS

Here, a multi-structure LBP is proposed to define the facial expression of the facial image. For extracting the features, both circular and elliptical neighbourhoods were used. The four different structures: anisotropic microstructure, isotropic microstructure, anisotropic macrostructure and isotropic macrostructure are defined along with image pyramid technique. The experimental results on the JAFFE and CK databases illustrate the merits of the proposed technique. The size of the images affect the performance of proposed technique as smaller images can provide large macrostructures.

REFERENCES

- [1] A.Mehrabian, Communication without words, Psychology Today, vol.2, 1968, pp.53-55.
- [2] P. Ekman, W. V. Friesen, and J. C. Hager, Facial action coding system. A Human Face, Salt Lake City, 2002.
- [3] D.Freire, Smile detection using Local Binary Pattern and Support Vector Machine, in 4th International Conference on Computer Vision Theory and Applications,2002.
- [4] J.Whitehill, G.Littlewort, I.Fasel,M.Barlett and J.Movellan, Toward Practicle Smile Detection, *IEEE Transactions on Pattern Analysis and Machine Intelligence*, 31(11),2009,pp.2106-2111.
- [5] C.Shan, Smile Detection by Boosting Pixel Differences, *IEEE Transactions on Image Processing*, 21(1), 2012, pp.431-436.
- [6] Q.Ji,Z.Zhu, and P.Lan, Real-time nonintrusive monitoring and prediction of driver fatigue, *IEEE Transactions on Vehicle Technology*,53(4), 2004, pp.1052-1068.
- [7] B. Gholami, W. M. Haddad, and A. R. Tannenbaum, Relevance Vector Machine Learning for Neonate Pain Intensity Assessment Using Digital Imaging, *IEEE Trans. Biomed. Eng.* 57(6), 2010, 1457–1466.
- [8] B. Fasel and J. Luetttin, Automatic facial expression analysis: A survey, *Pattern Recognition*, 36(1), 2003, pp. 259–275.
- [9] Z. Zeng, M. Pantic, G. I. Roisman, and T. S. Huang, A survey of affect recognition methods: Audio, visual, and spontaneous expressions, *IEEE Trans. Pattern Anal. Mach. Intelligence*, 31(1), 2009, pp. 39–58.



- [10] M. Pantic and I. Patras, Dynamics of facial expression: Recognition of facial actions and their temporal segments from face profile image sequences, *IEEE Trans. Syst. Man, Cybern. Part B Cybern.* 36(2), 2006, pp. 433–449.
- [11] T. R. Almaev and M. F. Valstar, Local Gabor Binary Patterns from three orthogonal planes for automatic facial expression recognition, in Humaine Association Conference on Affective Computing and Intelligent Interaction, 2013, pp. 356–361.
- [12] Tsai D.M and Huang T.Y, Automated surface inspection for statistical textures,*Image Vis Comput* 21(4), 2003, pp.307–323.
- [13] Chun Y.D, Kim N.C and Jang I.H, Content-based image retrieval using multiresolution color and texture features,*IEEE TransMultimed* 10(6), 2008, pp.073–1084.
- [14] Ji Q, Engel J andCraine E, Texture analysis for classification of cervix lesions,*IEEE Trans Med Imaging* 19(11), 2000, pp.1144–1149
- [15] Haralick R.M, Shanmugam Kand Dinstein I, Textural features for image classification,*IEEE Trans Syst Man Cybern* 3(6), 1973, pp.610–621
- [16] Laine A and Fan J, Texture classification by wavelet packet signatures, *IEEE Trans Pattern Anal Mach Intell*, 15(11),1993, pp.1186–1191.
- [17] Manjunath B.S, Ma W.Y, Texture features for browsing and retrieval of image data,*IEEE Trans Pattern Anal Mach Intell*, 18(8), 1996, pp.837–842.
- [18]. Randen T andHusoy J, Filtering for texture classification: a comparative study,*IEEE Trans Pattern Anal Mach Intell*, 21(4), 1999, pp. 291–310.
- [19] Leung T and Malik J, Representing and recognizing the visual appearance of materials using three-dimensional textons, *Int J Comput Vis*, 43(1), 2001, pp.29–44.
- [20] Schmid C, Constructing models for content-based image retrieval, In: Proceedings of Conference on Computer Vision and Pattern Recognition. Montbonnot, France, pp 39–45,2001.
- [21] Varma M and , Zisserman A, A statistical approach to texture classification from single images,*Int J Comput Vis*, 62(1), 2005, pp.61–81
- [22] Ojala T, Valkealahti K, Oja Eand Pietikaˆinen M, Texture discrimination with multidimensional distributions of signed gray-level differences,*Pattern Recognition*, 34(3), 2001, pp.727–739.
- [23] Maˆenpaˆaˆ Tand Pietikaˆinen M, Texture analysis with local binary patterns, In: Chen C, Wang P (eds) Handbook of Pattern Recognition and Computer Vision. 3rdedn. World Scientific, Singapore, pp 197–216,2005.
- [24] Zhang J and Tan T, Brief review of invariant texture analysis methods,*Pattern Recognition*, 35(3), 2002, pp.735–747.
- [25] Heikkilaˆ M, Pietikaˆinen M and Schmid C, Description of interest regions with local binary patterns,*Pattern Recognition*, 42(3), 2009, pp.425–436.
- [26]. Ahonen T, Hadid Aand Pietikaˆinen M, Face description with local binary patterns: application to face recognition,*IEEE Trans Pattern Anal Mach Intell*, 28(12), 2006, pp.2037–2041.



- [27] Liao S, Chung A (2007) Face recognition by using elongated local binary patterns with average maximum distance gradient magnitude, In: Proceedings of Asian Conference on Computer Vision. Tokyo, Japan, pp 672–679
- [28] Xiaoyang T and Triggs B, Enhanced local texture feature sets for face recognition under difficult lighting conditions, *IEEE Trans Image Process* 19(6), 2010, pp.1635–1650.
- [29] Zhang W, Shan S, Qing L, Chen X and Gao W, Are Gabor phases really useless for face recognition?, *Pattern Anal Appl*, 12(3), 2009, pp.301–307
- [30] Ma'empa'a' T, Ojala T, Pietika'inen M, Soriano M (2000) Robust texture classification by subsets of local binary patterns, In: Proceedings of International Conference on Pattern Recognition. Barcelona, Spain, pp 947–950
- [31] Ojala T, Pietika'inen M and Ma'empa'a' T, Multiresolution grayscale and rotation invariant texture classification with local binary patterns, *IEEE Transform Pattern Anal Mach Intell*, 24(7), 2002, pp.971–987.
- [32] Shu L, Law Mand Chung A, Dominant local binary patterns for texture classification, *IEEE Trans Image Process*, 18(5), 2009, pp.1107–1118.
- [33] Ahonen T, Matas J, He C and Pietika'inen M, Rotation invariant image description with local binary pattern histogram fourier features, In: Proceedings of 16th Scandinavian Conference on Image Analysis. Oslo, Norway, pp 61–70, 2009.
- [34] Guo Z, Zhang L and Zhang D, Rotation invariant texture classification using LBP variance (LBPV) with global matching, *Pattern Recognition*, 43(3), 2010, pp.706–719.
- [35] Guo Z, Zhang L and Zhang D, A completed modeling of local binary pattern operator for texture classification, *IEEE Trans Image Process*, 19(6), 2010, pp.1657–1663.
- [36] Zhao G and Pietika'inen M, Dynamic texture recognition using local binary patterns with an application to facial expressions, *IEEE Trans Pattern Anal Mach Intelligence*, 29(6), 2007, pp.915–928.
- [37] Ma'empa'a' Tand Pietika'inen M, Multi-scale binary patterns for texture analysis, In: Proceedings of Scandinavian Conference on Image Analysis. Halmstad, Sweden, 2003, pp 885–892.
- [38] Turtinen M and Pietika'inen M, Contextual analysis of textured scene images, In: Proceedings of British Machine Vision Conference. Edinburgh, UK, 2006, pp 849–858.
- [39] Qian X, Hua X-S, Chen P and Ke L, PLBP: an effective local binary patterns texture descriptor with pyramid representation, *Pattern Recognition*, 44(10), 2011, pp.2502–2515.
- [40] Nanni L, Lumini A and Brahmam S, (2010) Local binary patterns variants as texture descriptors for medical image analysis, *Artificial Intell Med*, 49(2), 2010, 117–125.
- [41] He Y, Sang N and Gao C, Pyramid-based multi-structure local binary pattern for texture classification, In: Proceedings of Asian Conference on Computer Vision. Queenstown, New Zealand, 2010, pp 133–144
- [42] Lowe D, Distinctive image features from scale-invariant keypoints, *Int J Comput Vis*, 60(2), 2004, 91–110.
- [43] Lazebnik S, Schmid Cand Ponce J, A sparse texture representation using local affine regions, *IEEE Trans Pattern Anal Mach Intell*, 27(8), 2005, pp.1265–1278

- [44] T. Kanade, J. F. Cohn, and Y. Tian, "Comprehensive database for facial expression analysis," in *4th IEEE International Conference on Automatic Face and Gesture Recognition*, 2000, pp. 46–53.
- [45] M. J. Lyons, "Automatic classification of single facial images," *IEEE Transactions on Pattern Analysis and Machine Intelligence*, vol. 21, no. 12, 1999, pp. 1357–1362.
- [46] S. L. Happy and A. Routray, "Automatic facial expression recognition using features of salient facial patches," *IEEE Transactions on Affective Computing*, vol. 6, no. 1, 2015, pp.1–12.
- [47] C. Shan, S. Gong, and P. W. Mcowan, "Facial expression recognition based on Local Binary Patterns : A comprehensive study," *Image and Vision Computing*, vol. 27, no. 6, 2009, pp. 803–816.
- [48] T. Jabid, M. H. Kabir, and O. Chae, "Robust facial expression recognition based on local directional pattern," *ETRI Journal*, vol. 32, no. 5, 2010, pp. 784–794.
- [49] R. Jiang, A. T. S. Ho, I. Cheheb, N. Al-Maadeed, S. Al-Maadeed, and A. Bouridane, "Emotion recognition from scrambled facial images via many graph embedding," *Pattern Recognition*, vol. 67, 2017, pp. 245–251.
- [50] M. Z. Uddin, M. M. Hassan, A. Almogren, A. Alamri, M. AlRubaian, and G. Fortino, "Facial Expression Recognition Utilizing Local Direction-based Robust Features and Deep Belief Network," *IEEE Access*, vol. 5, 2017, pp. 1–9.